Cell

Feedback Control of Gene Expression Variability in the *Caenorhabditis elegans* Wnt Pathway

Ni Ji,[1,5] Teije C. Middelkoop,[3,5] Remco A. Mentink,[3] Marco C. Betist,[3] Satto Tonegawa,[4] Dylan Mooijman,[3] Hendrik C. Korswagen,[3,*] and Alexander van Oudenaarden[2,3,*]

[1]Department of Brain and Cognitive Sciences, Massachusetts Institute of Technology, 77 Massachusetts Avenue, Cambridge, MA 02139, USA

[2]Department of Physics and Department of Biology, Massachusetts Institute of Technology, 77 Massachusetts Avenue, Cambridge, MA 02139, USA

[3]Hubrecht Institute, Royal Netherlands Academy of Arts and Sciences and University Medical Center Utrecht, Uppsalalaan 8, 3584 CT Utrecht, the Netherlands

[4]Milton Academy, 170 Centre Street, Milton, MA 02186, USA

[5]These authors contributed equally to this work

*Correspondence: r.korswagen@hubrecht.eu (H.C.K.), a.vanoudenaarden@hubrecht.eu (A.v.O.)

http://dx.doi.org/10.1016/j.cell.2013.09.060

SUMMARY

Variability in gene expression contributes to phenotypic heterogeneity even in isogenic populations. Here, we used the stereotyped, Wnt signaling-dependent development of the *Caenorhabditis elegans* Q neuroblast to probe endogenous mechanisms that control gene expression variability. We found that the key Hox gene that orients Q neuroblast migration exhibits increased gene expression variability in mutants in which Wnt pathway activity has been perturbed. Distinct features of the gene expression distributions prompted us on a systematic search for regulatory interactions, revealing a network of interlocked positive and negative feedback loops. Interestingly, positive feedback appeared to cooperate with negative feedback to reduce variability while keeping the Hox gene expression at elevated levels. A minimal model correctly predicts the increased gene expression variability across mutants. Our results highlight the influence of gene network architecture on expression variability and implicate feedback regulation as an effective mechanism to ensure developmental robustness.

INTRODUCTION

Gene expression is inherently variable, even among isogenic cells situated in identical environments (Raj and van Oudenaarden, 2008; Raj et al., 2008; Eldar and Elowitz, 2010; Balázsi et al., 2011; Li and Xie, 2011). On the one hand, variability in gene expression may confer beneficial phenotypic diversity. For example, it may serve as a "bet-hedging" strategy for isogenic microbial populations to ensure survival in fluctuating environments (Thattai and van Oudenaarden, 2004; Kussell and Leibler, 2005; Wolf et al., 2005; Acar et al., 2008; Beaumont et al., 2009; Eldar et al., 2009) or as a "symmetry-breaking" mechanism to induce multiple cell fates from a single progenitor cell type (Wernet et al., 2006; Chang et al., 2008; Kalmar et al., 2009). On the other hand, excessive variability in gene expression could disrupt normal development and tissue maintenance, leading to aberrant phenotypes (Aranda-Anzaldo and Dent, 2003; Chung and Levens, 2005; Henrichsen et al., 2009; Raj et al., 2010). The remarkable robustness of numerous physiological events implies that endogenous mechanisms must exist to effectively control variability in gene expression (Nijhout, 2002; Félix and Wagner, 2008; Boettiger and Levine, 2013).

In a simple model of constitutive gene expression, the equilibrium level of messenger RNA (mRNA) transcripts is expected to follow a Poisson probability distribution. A distinct feature of the Poisson distribution is that the ratio between the variance and the mean, termed the Fano factor, equals exactly one, regardless of the detailed parameters. For genes under transcriptional regulation, substantial deviations from the Poisson behavior have been theoretically proposed (Kepler and Elston, 2001; Friedman et al., 2006; Shahrezaei and Swain, 2008) and experimentally observed in a series of studies (Golding et al., 2005; Cai et al., 2006; Raj et al., 2006; Zenklusen et al., 2008). Such deviation has often been attributed to transcriptional bursting, where the promoter transitions stochastically between its active and inactive states. In addition, fluctuation in the abundance of the upstream regulators can also propagate to increase the variability of the target gene expression (Hooshangi et al., 2005; Pedraza and van Oudenaarden, 2005; Rosenfeld et al., 2005; Dunlop et al., 2008).

Pioneering theoretical and synthetic biology studies have highlighted the potential of regulatory networks in controlling gene expression variability. Negative feedback, a common mode of regulation, has been shown to suppress variability in synthetic gene expression systems (Becskei and Serrano, 2000; Austin et al., 2006). Positive feedback has been extensively studied for its ability to induce multimodal or

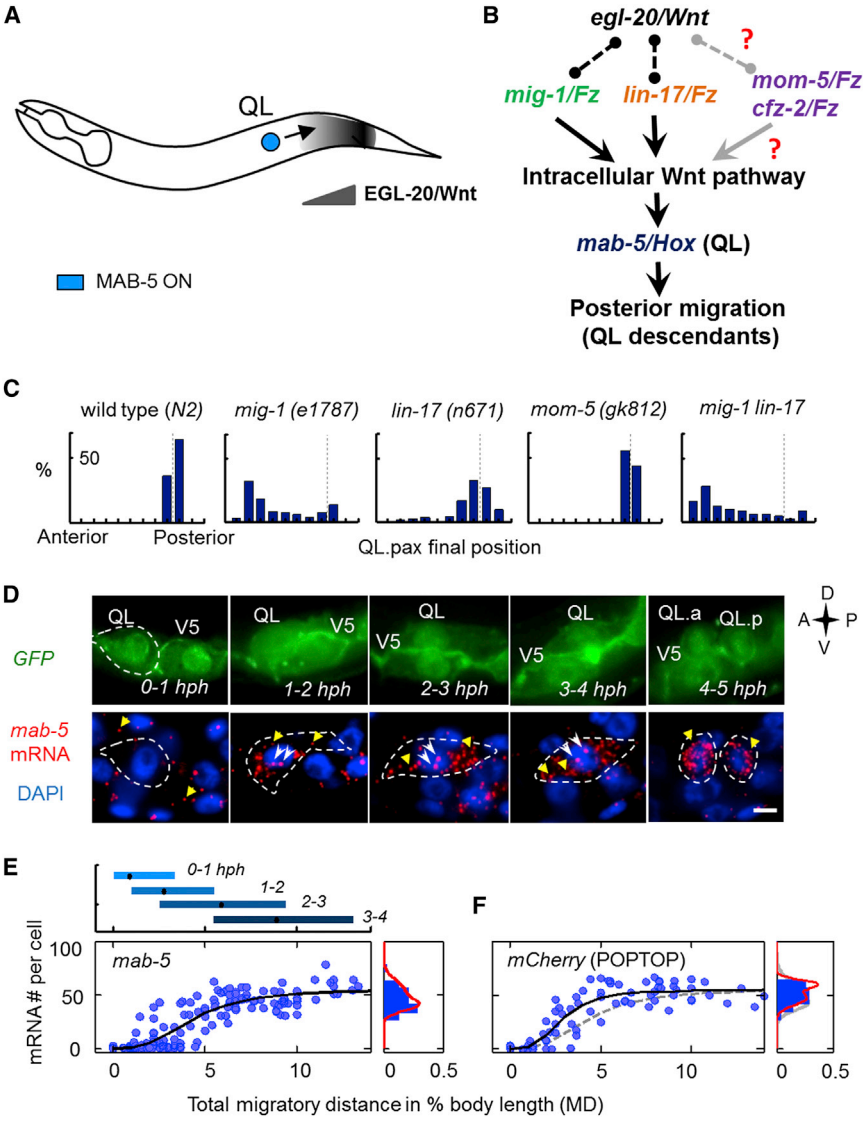

Figure 1. Using Single-Cell Transcript Counting to Study the Control of *mab-5* Expression

(A) Schematic representation of the activation of MAB-5 expression in QL in response to the posterior-to-anterior gradient of EGL-20/Wnt.

(B) Model of Wnt signaling based on published studies. Question marks and gray edges indicate lack of definitive evidence.

(C) Final position of QL descendants in wild-type and various Frizzled loss-of-function mutants. Unless otherwise noted, compound mutants carry the same alleles as single mutants.

(D) Detection of *mab-5* transcripts using smFISH over the course of QL migration. Upper: QL at different stages of its migration. V5 is a stationary cell used as spatial reference. Lower: smFISH staining of *mab-5* transcripts in the same cells as shown above. Yellow arrowheads: single *mab-5* transcripts; white arrowheads: transcription centers in the nucleus. Scale bar represents 2.5 μm.

(E) *mab-5* transcription dynamics in single QL neuroblasts in wild-type animals. Upper: normalized total MD for worms collected at different time points after hatching. Black dots mark the mean, and blue bars span 2.5–97.5 percentiles. Lower: number of *mab-5* transcripts per cell plotted against MD. The histogram to the right is generated using data points to the left with MD > 8. Black lines are generated by fitting to a sigmoidal function. Red curves are generated by fitting with two Gaussian distributions.

(F) *mCherry* transcription dynamics in the POPTOP strain.

See also Figure S1.

"switch-like" behavior in both synthetic and endogenous systems (Becskei et al., 2001; Xiong and Ferrell, 2003; Ozbudak et al., 2004; Acar et al., 2005; Weinberger et al., 2005; To and Maheshri, 2010). In contrast to the simplicity of synthetic circuits, endogenous genes are embedded in densely connected networks with mixed feedback loops and multilayered cascades (Milo et al., 2002; Davidson, 2010; Hirsch et al., 2010). Whether and how regulatory networks regulate gene expression variability endogenously remain to be explored.

Caenorhabditis elegans provides an excellent model for studying the endogenous control of gene expression variability. Its highly stereotyped development (Sulston and Horvitz, 1977) implicates underlying mechanisms that robustly control transcriptional variability. Here, we study specifically the stereotyped migratory decision of the *C. elegans* Q neuroblast. Two Q neuroblasts, QL and QR, are born at bilaterally symmetrical positions in the *C. elegans* embryo but migrate oppositely along the anterior-posterior axis upon hatching (Figure 1A). In the left Q neuroblast (QL), expression of the Hox gene *mab-5*/*Antennapedia* is necessary and sufficient to ensure the posterior migration of the QL descendants. In the right Q neuroblast (QR), however, the absence of *mab-5* expression drives the cell to migrate toward the anterior (Salser and Kenyon, 1992; Harris et al., 1996). In wild-type animals, *mab-5* expression in QL is dependent on the canonical Wnt signal transduced through the posteriorly produced Wnt ligand, EGL-20 (Figures 1A and 1B; Whangbo and Kenyon, 1999; Coudreuse et al., 2006). Two out of the four *C. elegans* Frizzled type Wnt receptors, MIG-1 and LIN-17, are required for *mab-5* expression in QL (Harris et al., 1996). The other Frizzled homologs, *mom*-5 and *cfz-2*, have also been implicated in the regulation of the migration of QL descendants (Zinovyeva et al., 2008). Interestingly, Frizzled mutants exhibit varying degrees of partially penetrant migratory defects, where a fraction of QL descendants reverse to migrate anteriorly (Zinovyeva et al., 2008; Figures 1C and S1A available online). Whether this phenotypic heterogeneity originates at or downstream from *mab-5* expression is unclear.

By combining single-cell transcript counting with genetic manipulation, we identified a strong link between the variability

in *mab-5* expression and the penetrance of the migratory phenotype. We observed a complex relationship between the variability and the mean levels of *mab-5* expression, implicating feedback regulation. A systematic search for regulatory interactions revealed a network of positive and negative feedback loops between the Frizzled receptors and the Wnt signaling pathway. A minimal network model captures the variability in *mab-5* expression across mutants and provides mechanistic insights on how the wild-type network achieves robustness. Our results demonstrate, in a developmentally relevant context, the contribution of a regulatory network to controlling gene expression variability.

RESULTS

Wnt Signaling Activates *mab-5* Expression to a Stable Range in Wild-Type QL

To explore the putative relation between *mab-5* expression and the phenotypic heterogeneity in the Wnt pathway mutants, it is necessary to quantitatively compare *mab-5* expression between wild-type and mutants. We started by characterizing *mab-5* expression in the wild-type QL neuroblasts (Figures 1D and 1E). Using *s*ingle *m*olecule *f*luorescent *i*n *s*itu *h*ybridization (smFISH, Raj et al., 2008), we counted *mab-5* transcripts at various stages of QL migration (Figure 1D). The total migratory distance (MD) of QL and QR (Figure 1E, top, and Figure S1B) was used as an indicator of migratory stage. Data from many single QL cells were combined to obtain a population profile of *mab-5* expression dynamics (Figure 1E, bottom).

Before the onset of migration, *mab-5* transcripts were present at low levels in QL (Figures 1D and 1E, MD = 0–2). Thereafter, QL began to polarize, and *mab-5* transcripts started to appear in the cytoplasm. Concurrently, nascent transcripts began to cumulate in the nucleus as bright transcription centers (TCs, Figures 1D and S1C). The frequent appearance of paired TCs likely indicates heightened transcriptional activity on both alleles (Raj et al., 2006). After a period of initial variability, *mab-5* expression converged to around 50–60 transcripts per cell (MD $\geq$ 8, Figure 1E). The variability in *mab-5* expression stabilized to a Fano factor of 2.4. This value is greater than the average measurement of 1.6 in *Escherichia coli* (Taniguchi et al., 2010) yet is over 10-fold lower than those reported for mammalian mRNAs (Raj et al., 2006).

Although Wnt signaling has been suggested as the main activator of *mab-5* transcription (Korswagen, 2002), whether it acts directly within QL remains uncertain. We probed the cell-autonomous role of Wnt signaling by blocking it either globally or Q cell specifically using a dominant-negative form of POP-1/TCF (*DN-pop-1*) (Korswagen et al., 2000). In both mutants, we observed a more than 95% reduction in *mab-5* transcripts in QL (Figure S1D), confirming a cell-autonomous role of Wnt signaling in activating *mab-5* expression.

The above finding suggests that *mab-5* expression may serve as an endogenous readout of Wnt pathway activity in QL. To confirm this possibility, we first compared the transcription dynamics of *mab-5* to that of a *mCherry* transgene driven by a *pes-10* minimal promoter with seven POP-1 binding sites (POP-1 and TCF Optimal Promoter [POPTOP]; Green et al., 2008). The dynamics of *mCherry* transcripts closely resembled that of *mab-5* (Figures 1E and 1F). Furthermore, mutation of a conserved TCF binding motif in the *mab-5* promoter (K. Cadigan, personal communication) led to a significant reduction in reporter transgene expression (Figures S1E and S1F). Taken together, these observations motivate the use of *mab-5* transcript level as an endogenous readout of Wnt signaling in QL.

Three Frizzled Receptors Are Expressed in QL and Exhibit Distinct Expression Dynamics

Because mutation of different Frizzled paralogs leads to different penetrance in migratory phenotype (Figures 1C and S1A), we speculated that, apart from their difference in functional efficacy, individual Frizzled paralogs may be expressed at different levels in QL. To test this, we used paralog-specific smFISH to quantify the expression of the four Frizzled receptors in QL. QL-specific expression was detected for *mig-1*, *lin-17*, and *mom-5*, but not for *cfz-2* (Figures 2A and S2A). In addition to difference in average abundance, these paralogs also differed in their temporal patterns of expression. *mig-1* transcripts decreased from an average of 27 copies per cell to less than 10 over the course of migration. *lin-17*, on the opposite, rose from less than 10 copies per cell to an average of 34. *mom-5* was expressed at less than 10 copies per cell throughout QL migration (Figure S2A). Outside QL, the four Frizzleds also exhibited distinct global expression patterns (Figure S2B).

Intuitively, a positive correlation may be expected between the expression of a receptor and that of its signaling target. A negative correlation was, however, observed between the abundance of *mig-1* transcripts and that of *mab-5* (Figure 2B, Pearson's $R = -0.67$, $p < 0.001$). Compared to *mig-1*, mutation of *lin-17* leads to a weaker migratory defect (Figure 1C). However, a strong positive correlation was observed between *lin-17* and *mab-5* transcripts at the single-cell level (Pearson's $R = 0.91$, $p < 0.001$). No significant correlation was observed between *mom-5* and *mab-5* (Pearson's $R = 0.02$, $p > 0.5$). Together, the distinct transcriptional and correlation profiles suggest that divergent transcriptional regulatory programs exist upstream of the Frizzled receptors.

Frizzled Mutants Exhibit Different Degrees of Variability in *mab-5* Expression

Having assessed *mab-5* and Frizzled expression in the wild-type, we next asked how *mab-5* expression is affected by mutations in the Frizzled receptor genes. Previously, reduction in MAB-5 antibody staining has been reported in *mig-1* and *lin-17* single mutants (Harris et al., 1996). In agreement, we observed a strong reduction in *mab-5* transcripts in QL in most of *mig-1(e1787)* single mutants (Figure 3A). A small fraction of QLs, however, retained significant levels of *mab-5* expression (20 transcripts per cell or higher). Cell-to-cell heterogeneity was also evident in the *lin-17(n671)* single mutant. Individual QLs exhibited between very low to a near-wild-type amount of *mab-5* transcripts. The *mom-5(gk812)* mutant, unlike the wild-type, exhibited high variability in *mab-5* expression beyond the initial phase of QL migration (MD > 5, note cells with <25 copies of *mab-5*). In comparison, *mab-5* levels in the *cfz-2(ok1201)* mutant were indistinguishable from the wild-type.

Homozygous mutation in two or more of the three Frizzled receptors (*mig-1*, *lin-17*, and *mom-5*) resulted in nearly

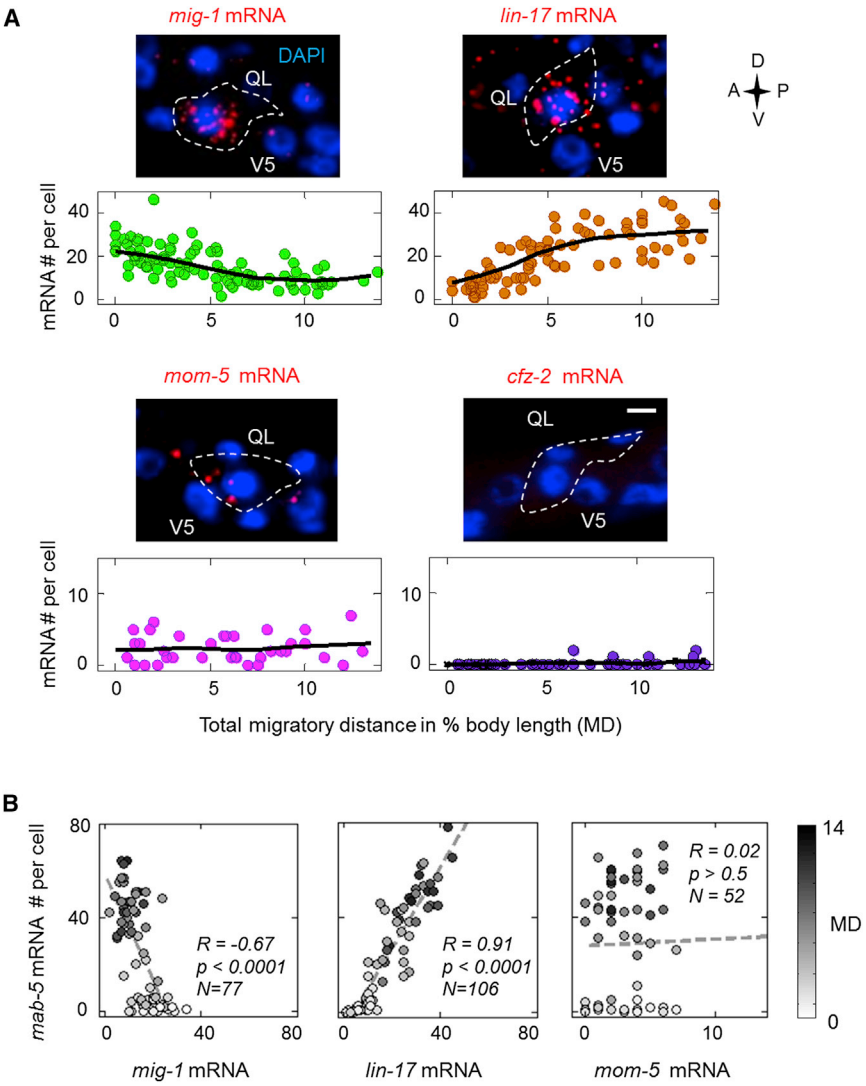

Figure 2. Three Frizzled Paralogs Are Dynamically Transcribed in QL

(A) smFISH staining and single-cell transcript counts for the four *C. elegans* Frizzled paralogs over the course of QL migration.

(B) Single-cell correlation between Frizzled and *mab-5* transcript counts. Shades of dots indicate corresponding MD value.

See also Figure S2.

complete loss of *mab-5* expression in QL (Figure 3A). In contrast, heterozygotes of these mutants exhibited similar average *mab-5* levels as the wild-type. Interestingly, heterozygotes of the Frizzled triple mutant (triple het) showed increased variability in *mab-5* expression, where a small fraction of late-stage QLs contained less than 20 *mab-5* transcripts (Figure 3A). This observation, together with those from the single mutants, indicates that partial reduction of Frizzled receptor function could disrupt the reliable activation of *mab-5* transcription in QL.

Motivated by the recent discovery that variability in gene expression underlies partial penetrance (Raj et al., 2010), we questioned whether variability in *mab-5* transcript level is predictive of the phenotypic penetrance of different mutants. We hypothesized that *mab-5* expression must exceed a certain threshold to prevent the QL descendants from migrating anteriorly. Under this hypothesis, we searched (Figure S3C) and found threshold values of around 25 transcripts per cell (Figure 3C) to yield accurate predictions of the phenotypic penetrance. *mom-5* single and compound mutants were not included in this analysis due to the *mab-5*-independent requirement of *mom-5* for anterior migration (Zinovyeva et al., 2008). Thus, upregulating *mab-5* expression above a certain threshold may be critical in driving robust migratory decisions of the QL descendants.

Perturbing EGL-20 and MAB-5 Function Increases Variability in *mab-5* Expression

To test whether the increase in *mab-5* variability is unique to the Frizzled mutants, we next perturbed the input to the Wnt pathway, the EGL-20/Wnt gradient. We used the *vps-29 (tm1320)* mutant in which destabilization of the retromer complex leads to a shortened and reduced EGL-20 gradient (Coudreuse et al., 2006). In these mutants, *mab-5* expression was reduced to below 25 transcripts per cell in around 10% of QLs (Figure 3B). The variability in *mab-5* expression was again predictive of the phenotypic penetrance: about 13% of the QL descendants were misplaced anteriorly (Figure 3C).

Conversely, we tested the effect of EGL-20 overexpression by expressing an EGL-20 transgene under the control of a heat shock promoter (Whangbo and Kenyon, 1999). The increased EGL-20 concentration (Figure S3B), however, did not significantly increase the average level of *mab-5* expression (Figure 3B, Mann-Whitney test, $p > 0.1$). Rather, *mab-5* expression in late-stage QLs appeared less variable (F test $p < 0.05$) than the wild-type. Although increased variability is frequently accompanied by reduced expression levels, this was not the case in the *smg-1(e1228); mab-5(e1239)* mutant (see Supplemental Information for motivations to use the *smg-1(e1228)* background). Instead, an increase in average *mab-5* level coincided with an increase in cell-cell variability (F test $p < 0.001$) (Figure 3B).

A Complex Relationship Exists between *mab-5* Variability and Average Expression Level

To quantitatively compare the variability in *mab-5* expression, we next calculated the Fano factor of *mab-5* transcript levels for both wild-type and mutants.

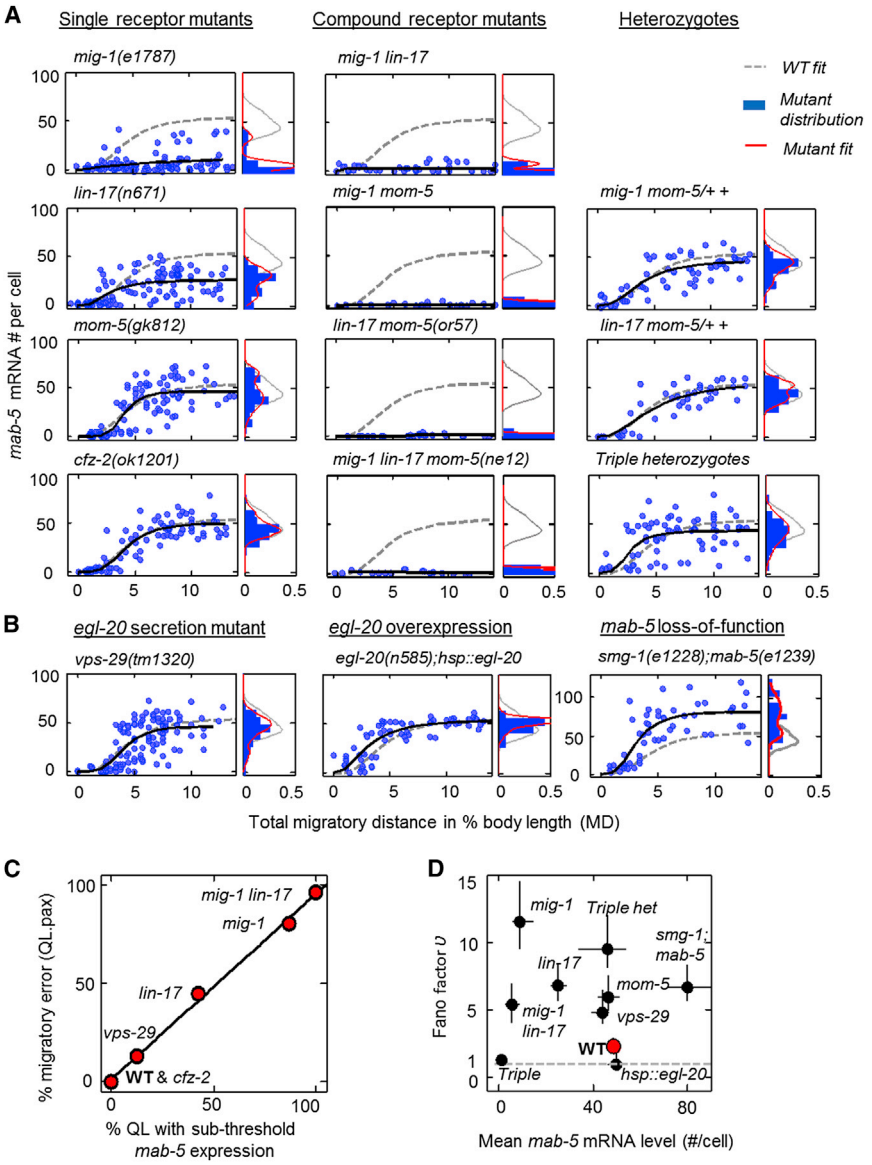

Figure 3. Wnt Signaling Mutants Exhibit Different Variability in *mab-5* Expression

(A) Dynamic and steady-state *mab-5* expression in Frizzled single and compound mutants.

(B) Dynamic and steady-state *mab-5* expression in mutants with altered EGL-20/Wnt gradient or loss of MAB-5 function.

(C) Correlation between *mab-5* transcript levels and the migratory phenotype of QL descendants in various Wnt pathway mutants. Same mutant alleles as listed in (A) and (B).

(D) Fano factor versus the steady-state mean of *mab-5*. Wild-type is marked in red. Gray broken line: Fano factor = 1. Error bars are 95% confidence intervals (CI).

See also Figure S3.

In most strains, Fano factors were initially high and decreased to stable values over the course of migration (Figure S3D). Plotting the steady-state Fano factor against the average transcript level revealed several interesting features (Figure 3D). First, Fano factor varied greatly across strains (range: 0.95–11.5). Thus, constitutive transcription with Poisson dynamics is insufficient to explain our observations. Alternatively, a model of bursty transcription would predict Fano factor to increase (if burst size is modulated) or decrease (if burst frequency is modulated) monotonically with the mean (Raser and O'Shea, 2004). However, the observed relation could not be summarized in a simple monotonic function (Figure 3D). Furthermore, whereas mutant QLs with reduced *mab-5* expression exhibited variable numbers of TCs (between 0 and 2) per nucleus, suggestive of bursty transcription (Figure S3E), the *smg-1;mab-5* mutant, which consistently exhibited two TCs per nucleus and high *mab-5* synthesis rate (Figures S3F and S3G), nonetheless showed increased variability in *mab-5* levels. As common models could not fully explain the complex relationship between *mab-5* variability and average expression level, other mechanisms, likely upstream of *mab-5* transcription, may play a role to influence *mab-5* expression variability.

All Three Frizzleds Are Transcriptional Targets of the Wnt Pathway

As *mab-5* expression consisted of distinct high and low subpopulations in a number of mutants (e.g., the *mig-1* single mutant and the triple heterozygotes), a feature attainable in systems with positive feedback (Becskei et al., 2001), we wondered whether feedback regulation exists within the Wnt pathway in QL. Although Wnt signaling is conventionally viewed as a feedforward cascade, evidence from nonnematode species suggests that feedback regulation exists and may play a role in Wnt pathway regulation (Cadigan et al., 1998; Sato et al., 1999; Willert et al., 2002).

To test whether Frizzled receptors are transcriptional targets of the Wnt pathway, we blocked Wnt signaling both globally and Q cell specifically. In both cases, we observed a more than 2-fold difference in the transcript levels of all three Frizzled genes (Figure 4A). In addition, the temporal dynamics of *mig-1* and *lin-17* transcription were lost in the mutants. Together, these observations indicate a role of feedback regulation in determining the levels and temporal dynamics of Frizzled expression (Figure 2A).

By ranking various Wnt signaling mutants by their average *mab-5* levels, we established a mutant series in which Wnt signaling level in QL varied in a graded manner (Figure 4B, left). In the majority of the strains, low levels of *mab-5* expression were consistently accompanied by low levels of *lin-17* and high levels of *mig-1* and *mom-5* and vice versa. These observations

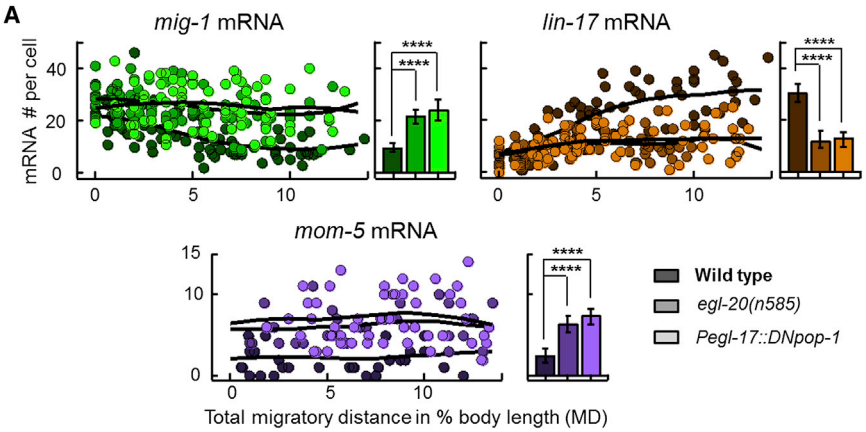

Figure 4. Frizzled Paralogs, *mig-1*, *lin-17*, and *mom-5*, Are Transcriptional Targets of the Wnt Pathway

(A) Dynamic and steady-state (MD > 8) Frizzled transcript levels in mutants with global or QL-specific blockade of EGL-20-dependent Wnt signaling. Same wild-type data as Figure 2A. ****$p < 0.0001$.

(B) Normalized expression levels of Frizzleds and *mab-5* in various genetic backgrounds. Only values significantly different from the wild-type (FDR corrected $p < 0.05$) were colored. Genotypes are indicated atop the bar graph with same mutant alleles as indicated previously. Error bars are 95% CI of the mean.

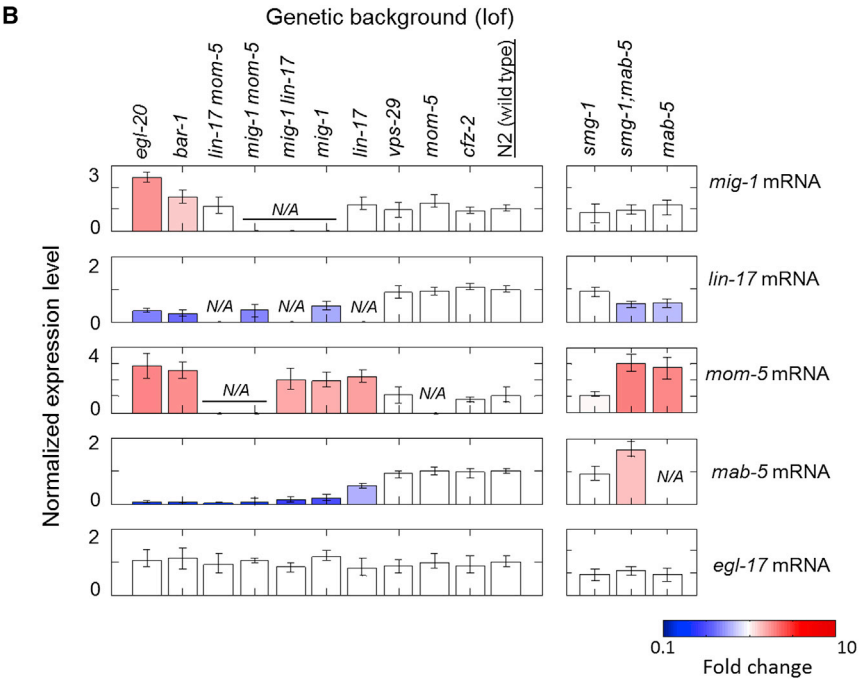

are again consistent with the notion of Frizzled receptors as transcriptional targets of Wnt signaling.

An exception to the above trend was found in the *smg-1; mab-5* mutants in which an increase in *mab-5* levels was observed with a concurrent increase in *lin-17* and a decrease in *mom-5* (Figure 4B, right). This exception suggests that functional MAB-5 is required for the feedback regulation of *lin-17* and *mom-5*. Meanwhile, the fact that *mig-1* expression remains unaltered in *mab-5* mutants suggests that the transcriptional feedback on *mig-1* is likely *mab-5* independent. Thus, both *mab-5*-dependent feedback and *mab-5*-independent feedback appear to exist in the Wnt signaling pathway in QL.

Interlocked Positive and Negative Feedback Loops Exist within the Wnt Pathway

We next sought to incorporate the feedback interactions into a network model of the Wnt pathway. With feedback, perturbation to a single gene can propagate to affect many genes in the network, making it difficult to deduce the immediate targets of the perturbed gene. We tackled this general challenge in network inference by employing *M*odular *R*esponse *A*nalysis (MRA, Bruggeman et al., 2002; Kholodenko et al., 2002) (Figure 5A). This algorithm is robust to unknown network components and reports only interactions between "closest neighbors" to avoid redundant reference to the same network structure.

Applying MRA to the average transcription profiles, we obtained a complex network of interlocked feedback loops (Figures 5B, 5C, and S4A–S4C). At the receptor level, positive feedback targeting *lin-17* and negative feedback targeting *mig-1* and *mom-5* are coupled by their shared dependence on Wnt signaling. Downstream of the Wnt pathway, *mab-5* not only mediates feedback to the Frizzleds but also negatively regulates its own transcription.

As Hox genes are master regulators with many transcriptional targets, we wondered whether *mab-5*, an *Antennapedia*-like Hox gene, regulates the expression of the Frizzled receptors and of itself by directly binding to the *cis*-regulatory regions of the respective genes. Previous chromatin immunoprecipitation sequencing (ChIP-seq) analysis (Niu et al., 2011) on L3 stage larvae has identified MAB-5 binding regions in the promoters and sometimes intronic regions of the above genes. To assess whether the same regions are also bound by MAB-5 during the time of Q neuroblast migration, we performed ChIP-qPCR on synchronized L1 animals, pulling down the GFP tag on the MAB-5::GFP fusion protein. Among the sequences tested, enrichment of MAB-5::GFP binding was specifically observed in the third intron of *mab-5* (Figure 5D). To confirm this, we built transgenic strains expressing *mCherry* under the control of both *mab-5* promoter and intronic sequences (Figure 5E, Supplemental Information). Interestingly, elimination of the MAB-5

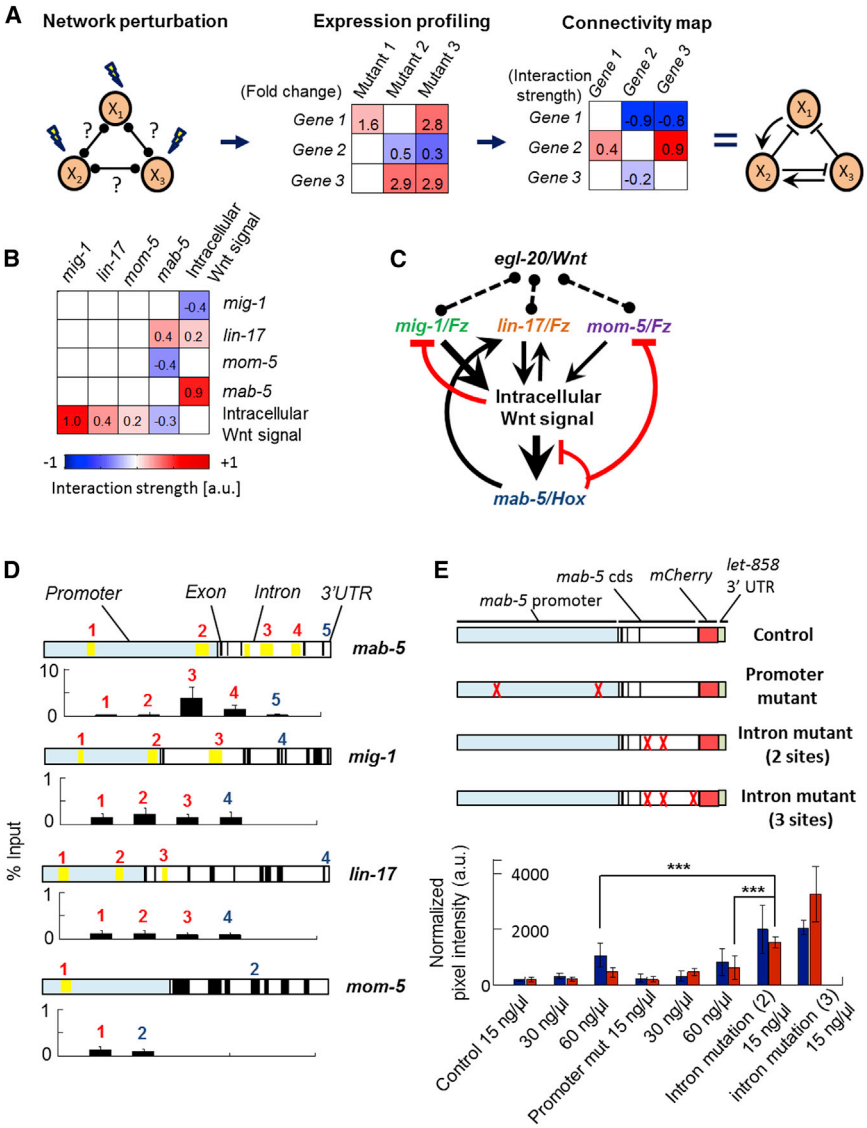

Figure 5. Inferring the Regulatory Network within the Wnt Pathway Using the MRA Algorithm

(A) Schematic of the work flow for implementing the MRA algorithm.

(B) Inferred connectivity matrix. Network components listed on top of the matrix represent putative regulators, and those listed on the right represent putative regulatory targets. Only significant (p value with Bonferroni correction < 0.05) interactions are colored based on the inferred interaction strengths.

(C) Revised Wnt pathway model based on the inference results.

(D) ChIP-qPCR reveals MAB-5::GFP binding to the intronic regions of the *mab-5* gene. Light blue: the promoter regions, where exons and introns are marked in black and white, respectively. Yellow: sequences enriched for MAB binding in the L3 stage (Niu et al., 2011). Numbers in red: locations of qPCR primers that target putative MAB-5 binding sites. Numbers in blue: locations of primers that target putative negative control regions (i.e., exonic or 3′ untranslated regions). n = 3 for all putative MAB-5 binding sites, and n = 2 for all negative control regions.

(E) Upper: schematic of the control and mutated reporter constructs carrying regulatory and coding sequences from the *mab-5* gene. Red crosses: sites of deletion. Lower: quantification of *mCherry* smFISH signal in QL neuroblasts in strains carrying reporters of *mab-5* regulatory sequence. Normalized pixel intensity is quantified as the sum of the top 20% pixel values in QL normalized by the average pixel intensity of single smFISH spots in the same image. Error bars are SDs of the mean. For each condition, two independent extrachromosomal lines (red and blue) were examined. n > 15 for each strain.

See also Figure S4.

binding regions specifically in the third intron induced a strong increase in *mCherry* expression both within (Figures 5E and S5E) and outside (Figure S4E) QL. Thus, the results from both approaches support a direct role of *mab-5* in repressing its own transcription. We additionally built reporter strains to test putative MAB-5 binding motifs in the regulatory regions of *lin-17* and *mom-5* (Figure S4F). However, no significant difference in transgene expression was found upon mutation of the selected motifs.

Positive and Negative Feedback Cooperate to Minimize Variability

To probe whether and how network topology influences the variability in *mab-5* expression, we constructed an ordinary differential equation (ODE) model of the inferred network (Table S1 and Supplemental Information). We first obtained model parameters by fitting the full 5-component model to average gene expression profiles (Figure S5A, Table S2, and Supplemental Information). The full model was then reduced to a one-dimensional (1D) model by exploiting time-scale differences (Figures 6A and S5B and Supplemental Information).

We then extended the deterministic model to a stochastic one and derived the expected Fano factor and mean level of the network output. To explore the general impact of network topology on the variability in its output, we modified the wild-type network to explore four different classes of topologies: those with no feedback, with negative feedback only (NFB only), with positive feedback only (PFB only), and with interlocked positive and negative feedback (IFB, Figure 6B). We then randomly varied the strengths (i.e., the half-activation threshold) and the amount of cooperativity of each feedback interaction between 0 to 10 times their wild-type values while keeping other parameters fixed.

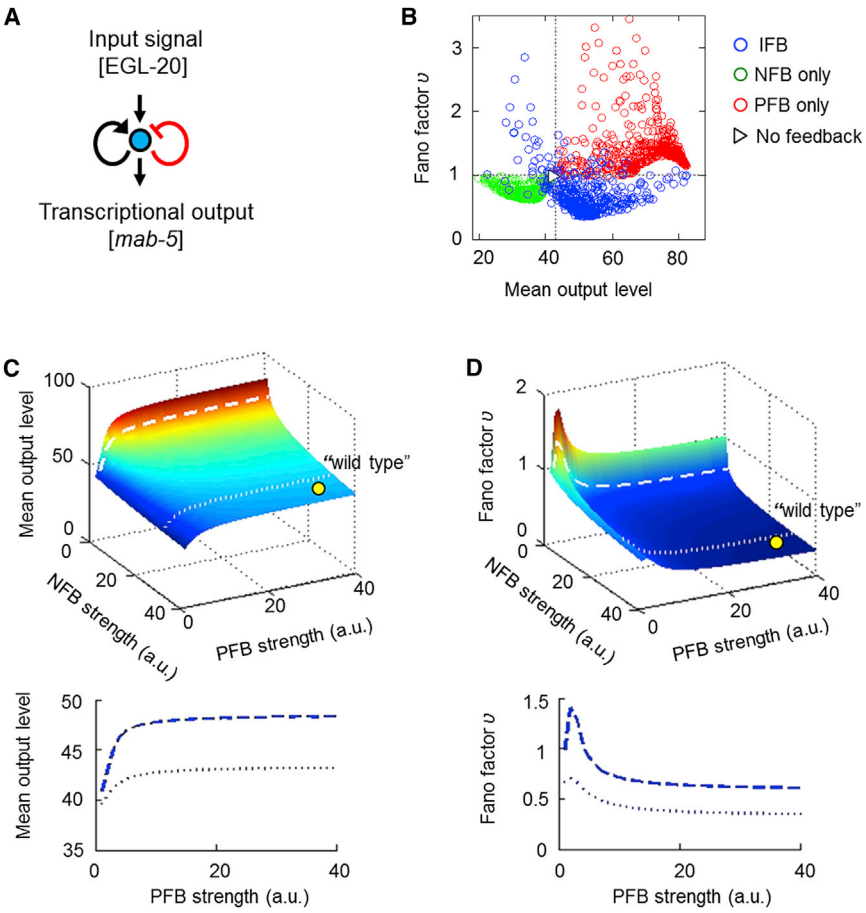

Figure 6. Modeling Reveals Synergistic Contribution of Positive and Negative Feedback in Reducing Output Variability

(A) Schematic of the reduced 1D model.

(B) Analytically derived Fano factor versus mean output values for networks with IFB, NFB only, PFB only, and no feedback.

(C) Upper: mean output value of the interlocked feedback network as a function of feedback strengths. Lower: replotting of the broken and dotted lines in the upper panel. Note difference in mean expression level at high PFB strength.

(D) Upper: Fano factor value of the interlocked feedback network as a function of feedback strengths. Lower: Replotting of the broken and dotted lines in the upper panel. Note the difference in Fano factor value at high PFB strength.

See also Figure S5 and Tables S1 and S2.

As illustrated in Figure 6B, different classes of networks occupied distinct domains of the Fano factor versus mean output space. Low output variability and low mean output levels were generally found in NFB-only networks, whereas the opposite was true for PFB-only networks. This variability versus mean trade-off was alleviated in networks with IFB. Many of the randomly sampled IFB networks occupied the lower right quadrant (i.e., low variability and high mean), a region hardly accessed by the other types of networks (see also Figure S5C).

We focused next on the IFB network and examined how output mean and variability depend on feedback strength. We found that output mean consistently decreased with strong negative feedback and increased with strong positive feedback. The effect of negative feedback was essentially compensated by positive feedback, resulting in intermediate mean values when both are strong (Figure 6C).

Meanwhile, output variability consistently decreased with strong negative feedback (Figure 6D; see also Figure S5E), which is consistent with results from synthetic circuits (Becskei and Serrano, 2000; Austin et al., 2006). With a fixed level of negative feedback, the extent to which variability was dampened, however, depends strongly on the strength of the positive feedback. While the Fano factor decreased to around 0.6 at low positive feedback strength, it rapidly dropped to less than 0.5 at high positive feedback strength (Figure 6D, dotted line). As a result, the lowest Fano factor values were found when both positive and negative feedback were strong. Thus, positive feedback indirectly promotes low variability by increasing the mean expression level (Figure S5D).

We additionally explored the dependence of output variability on the timescales at which the two types of feedback operate. Consistent with previous theoretical (Hornung and Barkai, 2008) and experimental studies (Austin et al., 2006), we found that Fano factor generally increased with fast positive feedback and with slow negative feedback (Figure S5F).

Model Predicts *mab-5* Variability in the Mutants

Because our network model was inferred and parameterized using average expression levels, we wondered whether it could predict the observed variability in *mab-5* expression. The observed variability likely originates from both intrinsic and extrinsic sources. To account for the latter, we included a parameter (D) to describe the effect of extrinsic fluctuations and determined its magnitude by fitting to the wild-type *mab-5* distribution (Supplemental Information). Remarkably, the revised model not only captured the distribution of *mab-5* levels in the wild-type but also predicted the changes in *mab-5* variability in various Wnt pathway mutants (Figures 7A, 7B, and S6A). Thus, alterations in network topology likely underlie the changes in *mab-5* variability across the mutants. Conversely, the wild-type network may contribute strongly to the observed low variability in *mab-5* expression.

Together, our results support a model in which variability in gene expression is controlled through a network of interlocked positive and negative feedback within the Wnt signaling pathway. The signal-amplifying effect of the positive feedback appears to be co-opted to ensure a strong negative feedback,

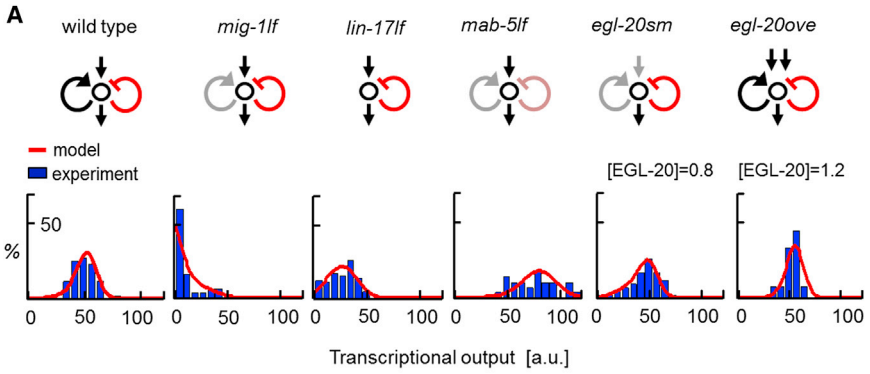

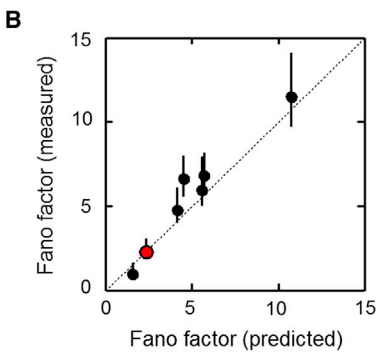

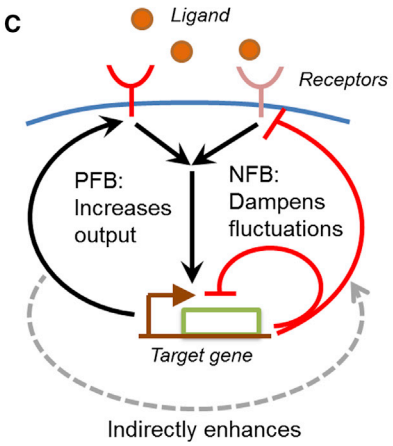

Figure 7. Model Predicts Variability in Various Strains

(A) Model prediction of the distribution of *mab-5* transcript levels in wild-type and various Wnt signaling mutants. Network diagrams indicate the speculated changes in network topology. Gray arrows indicate weakened interactions, and double arrows symbolize an increase in EGL-20 concentration. *egl-20sm*: *egl-20* secretion mutant; *egl-20ove*: *egl-20* overexpression mutant.

(B) Theoretically predicted versus the experimentally measured Fano factor values for the strains shown in (A). Error bars are 95% CI of the mean.

(C) Conceptual model of the interplay between the positive and the negative feedback in reducing variability.

See also Figure S6.

one that is needed to effectively dampen fluctuations in gene expression (Figure 7C). Increasing evidence of feedback regulation challenges the conventional notion of signaling pathways as linear, unidirectional cascades. It is likely the rule rather than the exception that feedback regulation is widely exploited in development and homeostasis to ensure robust control of gene expression.

DISCUSSION

Regulatory Network as an Endogenous Mechanism to Control Variability

Theoretical and synthetic studies over the past decade have provided "proof-of-principle" evidence that a regulatory network can be exploited to limit, tolerate, or amplify gene expression variability. Two common regulatory modules, positive feedback and negative feedback, have each been examined in detail. The joint action of the two, however, appears more complex (Acar et al., 2005; Brandman et al., 2005). Interlocked positive and negative feedback has been found to play a critical role in oscillatory systems (Ferrell et al., 2011). Our findings suggest that the same motif can be adapted to ensure stable gene expression at high levels. The versatility of the interlocked feedback motif exemplifies the rich potential of regulatory networks in implementing robust gene expression control.

Extrinsic versus Intrinsic Mechanisms in Controlling Gene Expression Variability

As regulatory networks often act upstream of the transcriptional machinery, they serve as "extrinsic" mechanisms in modulating transcriptional variability. In contrast, mechanisms that directly affect the assembly and release of the transcription machinery, such as promoter architecture (Boeger et al., 2008), chromatin organization (Weinberger et al., 2012), and the pausing of RNA polymerase II (Levine, 2011; Lagha et al., 2012), would serve as "intrinsic" mechanisms. Although both types of mechanisms have been extensively studied, how the two interact to influence gene expression variability is only beginning to be explored.

The results of this study implicate that extrinsic mechanisms may act through intrinsic mechanisms to modulate gene expression variability. Among the Wnt mutants we examined, a partial reduction in *mab-5* expression was often accompanied by a reduced and heterogeneous presence of transcription centers (Figure S3E). Thus, *mab-5* transcription may be inherently bursty, where the burst frequency and the burst size may be subject to modulation by extrinsic factors such as the Wnt signal. By promoting a strong Wnt signal, the regulatory network may efficiently reduce the burstiness and thereby dampen the variability in *mab-5* transcription. Mechanistically, a strong Wnt signal may allow BAR-1/β-catenin to reliably bind to POP-1/TCF, thus promoting robust release of polymerase II from the *mab-5* promoter region.

Cell-to-Cell Variability Carries Signatures of Network Topology

An emerging view in the study of stochastic gene expression argues that variability, or noise, can inform about the underlying mechanism of regulation (Cağatay et al., 2009; Chalancon et al., 2012; Munsky et al., 2012). In this study, we used average gene expression to infer network topology and found a surprising link between network topology and the variability in gene expression.

In retrospect, signatures of network topology may already be found in the variability in *mab-5* expression.

For example, low variability in the wild-type and the inability to increase *mab-5* level via EGL-20/Wnt overexpression suggest the existence of a negative feedback loop (Figures 3B and 3D). An experiment that eliminates the putative negative feedback was thus carried out to test this possibility (Figure 3B). Similarly, the distinct subpopulations of *mab-5* ON and OFF cells in strains such as the *mig-1* single mutant implicate the existence of positive feedback. Furthermore, we observed at the single-cell level a strong positive correlation between *lin-17* and *mab-5* levels in both the wild-type and multiple mutants in which both genes are intact (data not shown). This strong single-cell correlation may be attributed to a common upstream regulator (Dunlop et al., 2008) or a feedback loop. Both mechanisms turned out to exist in the inferred network (Figure 5C). Thus, cell-to-cell variability in gene expression may carry distinct signatures of the underlying network and serve as a useful guide to network identification.

EXPERIMENTAL PROCEDURES

C. elegans Strains and Culture

C. elegans strains were grown at 20°C using standard culture conditions. A full list of mutant alleles and transgenes are described in the Supplemental Information.

Scoring QL Descendent Migration

The precise positions of the Q descendants QL.pap/QL.paa were scored by DIC microscopy in late L1 stage larvae as described (Coudreuse et al., 2006).

Single-Molecule Fluorescence In Situ Hybridization

SmFISH was performed as described (Raj et al., 2008). Manual segmentation of GFP-marked QL periphery was performed, followed by automated spot counting in MATLAB-based custom-written software. Total MD was assayed by manually marking the nuclear position of QL and QR, tracing the A-P axis of the worm, and automatically computing the distance between QL and QR along the A-P axis. All smFISH probe sequences are listed in Table S3.

Heat Shock Activation of *hsp::egl-20*

Heat shock experiments were performed on *egl-20(n585)* animals carrying *muIs53 [hsp::egl-20; unc-22(dn)]* as described (Whangbo and Kenyon, 1999). Briefly, heat shock treatment was given to 0–0.5 hr synchronized L1 larvae in a total volume of 50 μl at 33°C for a desired length of time. Heat shock was terminated by chilling tubes on ice for 10 s, and worms were then grown on fresh plates at 20°C for an additional 2–2.5 hr.

ChIP-qPCR

Synchronized animals aged 3–5 hr posthatching were fixed in fresh 1% PFA for 30 min (Mukhopadhyay et al., 2008). Fixed samples were incubated with 400 μg/ml pronase in 0.1% SDS at 37°C for 15 min, followed by sonication and subsequent immunoprecipitation using the EpiTectChIP One-Day Kit (SABiosciences). Upon DNA elution, qPCR was performed immediately using the Phusion Master Mix (NEB). All ChIP-qPCR signals were normalized to total input DNA. qPCR primer sequences are listed in Table S4.

Cloning

mab-5 and Frizzled regulatory sequences were PCR amplified from N2 genomic DNA. To mutate putative MAB-5 binding motifs (11 bps) by base pair substitution, we used site-directed mutagenesis followed by gateway cloning to obtain transcriptional *mCherry* fusion constructs. To delete stretches of MAB-5 binding regions (<700 bp), we used yeast-mediated homologous recombination to clone genomic sequences and the *mCherry* coding sequence into the pNP30 vector (kind gift of N. Paquin). *Pegl-17::DN-pop-1* was made by cloning *DN-pop-1* from the *Phs::DN-pop-1* construct (Korswagen et al., 2000). Where feasible, transgenes were integrated into the genome as single copies using Mos1-mediated transgenesis as previously described (Frøkjaer-Jensen et al., 2008). See also the Extended Experimental Procedures.

Network Inference

Gene expression data from a defined window of QL migration (MD > 8) were used for network inference. All transcript counts were normalized to the wild-type mean, and the MRA algorithm (Kholodenko et al., 2002) was iteratively applied to bootstrap samples of the normalized data. The resulting distributions of interaction strengths were used to determine the significance of each putative interaction. See also the Extended Experimental Procedures.

Modeling

An ODE model was constructed based on the inferred network. Genetic interactions were described in Hill function form. Model parameters were obtained through nonlinear least square fitting to the gene expression data. The deterministic ODE model was extended to a Langevin-type stochastic model, from which Fano factors were analytically derived and numerically evaluated. See also the Extended Experimental Procedures for more details.

Statistical Analysis

The Mann-Whitney test was used to compare mean expression levels, and the F test was used to test equal variance between the wild-type and mutants. Nonparametric bootstrap was used to derive confidence intervals on average transcript counts and Fano factors values. The Benjamini-Hochberg procedure was used to achieve a false discovery rate (FDR) of less than 0.04 for comparison of transcript abundance; the Bonferroni correction with n = 20 was applied to the bootstrap p values of the inferred network interactions. Corrected p value of less than 0.05 was considered significant.

SUPPLEMENTAL INFORMATION

Supplemental Information includes Extended Experimental Procedures, six figures, and four tables and can be found with this article online at http://dx.doi.org/10.1016/j.cell.2013.09.060.

ACKNOWLEDGMENTS

This project was supported by the NIH/NCI Physical Sciences Oncology Center at MIT (U54CA143874), a NIH Pioneer award (DP1CA174420), an ERC Advanced grant (2011-294325_GeneNoiseControl) (A.v.O.), and a grant from the Dutch Cancer Society (HUBR 2008-4114) (H.C.K.). We thank N. Paquin for MosSCI cloning vector, N. Bhatla and Y. Zheng for help with strain construction, D. Grun for identifying enriched MAB-5 binding motifs, K. Cadigan for information on putative TCF binding sites, J. Goncalves and Y. Yuan for discussion on network inference, C. Kenyon, K. Shen, H. Sawa, H.R. Horvitz, and the Caenorhabditis Genetics Center (University of Minnesota, Minneapolis) for strains and transgenes, and we also thank H.R. Horvitz, J. Slotine, E. Nedivi, E. Sontag, D. Del Vecchio, G. Neuert, S. Itzkovitz, M. Bienko, and T. Okubo for critical discussion on the project.

Received: November 20, 2012
Revised: July 26, 2013
Accepted: September 27, 2013
Published: November 7, 2013

REFERENCES

Acar, M., Becskei, A., and van Oudenaarden, A. (2005). Enhancement of cellular memory by reducing stochastic transitions. Nature *435*, 228–232.

Acar, M., Mettetal, J.T., and van Oudenaarden, A. (2008). Stochastic switching as a survival strategy in fluctuating environments. Nat. Genet. *40*, 471–475.

Aranda-Anzaldo, A., and Dent, M.A. (2003). Developmental noise, ageing and cancer. Mech. Ageing Dev. *124*, 711–720.

Austin, D.W., Allen, M.S., McCollum, J.M., Dar, R.D., Wilgus, J.R., Sayler, G.S., Samatova, N.F., Cox, C.D., and Simpson, M.L. (2006). Gene network shaping of inherent noise spectra. Nature *439*, 608–611.

Balázsi, G., van Oudenaarden, A., and Collins, J.J. (2011). Cellular decision making and biological noise: from microbes to mammals. Cell *144*, 910–925.

Beaumont, H.J., Gallie, J., Kost, C., Ferguson, G.C., and Rainey, P.B. (2009). Experimental evolution of bet hedging. Nature *462*, 90–93.

Becskei, A., and Serrano, L. (2000). Engineering stability in gene networks by autoregulation. Nature *405*, 590–593.

Becskei, A., Séraphin, B., and Serrano, L. (2001). Positive feedback in eukaryotic gene networks: cell differentiation by graded to binary response conversion. EMBO J. *20*, 2528–2535.

Boeger, H., Griesenbeck, J., and Kornberg, R.D. (2008). Nucleosome retention and the stochastic nature of promoter chromatin remodeling for transcription. Cell *133*, 716–726.

Boettiger, A.N., and Levine, M. (2013). Rapid transcription fosters coordinate snail expression in the Drosophila embryo. Cell Rep. *3*, 8–15.

Brandman, O., Ferrell, J.E., Jr., Li, R., and Meyer, T. (2005). Interlinked fast and slow positive feedback loops drive reliable cell decisions. Science *310*, 496–498.

Bruggeman, F.J., Westerhoff, H.V., Hoek, J.B., and Kholodenko, B.N. (2002). Modular response analysis of cellular regulatory networks. J. Theor. Biol. *218*, 507–520.

Cadigan, K.M., Fish, M.P., Rulifson, E.J., and Nusse, R. (1998). Wingless repression of Drosophila frizzled 2 expression shapes the Wingless morphogen gradient in the wing. Cell *93*, 767–777.

Cağatay, T., Turcotte, M., Elowitz, M.B., Garcia-Ojalvo, J., and Süel, G.M. (2009). Architecture-dependent noise discriminates functionally analogous differentiation circuits. Cell *139*, 512–522.

Cai, L., Friedman, N., and Xie, X.S. (2006). Stochastic protein expression in individual cells at the single molecule level. Nature *440*, 358–362.

Chalancon, G., Ravarani, C.N.J., Balaji, S., Martinez-Arias, A., Aravind, L., Jothi, R., and Babu, M.M. (2012). Interplay between gene expression noise and regulatory network architecture. Trends Genet. *28*, 221–232.

Chang, H.H., Hemberg, M., Barahona, M., Ingber, D.E., and Huang, S. (2008). Transcriptome-wide noise controls lineage choice in mammalian progenitor cells. Nature *453*, 544–547.

Chung, H., and Levens, D. (2005). Minireview Molecules and c-myc Expression: Keep the Noise Down. Mol. Cell *20*, 157–166.

Coudreuse, D.Y.M., Roël, G., Betist, M.C., Destrée, O., and Korswagen, H.C. (2006). Wnt gradient formation requires retromer function in Wnt-producing cells. Science *312*, 921–924.

Davidson, E.H. (2010). Emerging properties of animal gene regulatory networks. Nature *468*, 911–920.

Dunlop, M.J., Cox, R.S., 3rd, Levine, J.H., Murray, R.M., and Elowitz, M.B. (2008). Regulatory activity revealed by dynamic correlations in gene expression noise. Nat. Genet. *40*, 1493–1498.

Eldar, A., and Elowitz, M.B. (2010). Functional roles for noise in genetic circuits. Nature *467*, 167–173.

Eldar, A., Chary, V.K., Xenopoulos, P., Fontes, M.E., Losón, O.C., Dworkin, J., Piggot, P.J., and Elowitz, M.B. (2009). Partial penetrance facilitates developmental evolution in bacteria. Nature *460*, 510–514.

Félix, M.A., and Wagner, A. (2008). Robustness and evolution: concepts, insights and challenges from a developmental model system. Heredity (Edinb) *100*, 132–140.

Ferrell, J.E., Jr., Tsai, T.Y.-C., and Yang, Q. (2011). Modeling the cell cycle: why do certain circuits oscillate? Cell *144*, 874–885.

Friedman, N., Cai, L., and Xie, X.S. (2006). Linking stochastic dynamics to population distribution: an analytical framework of gene expression. Phys. Rev. Lett. *97*, 168302.

Frøkjaer-Jensen, C., Davis, M.W., Hopkins, C.E., Newman, B.J., Thummel, J.M., Olesen, S.-P., Grunnet, M., and Jorgensen, E.M. (2008). Single-copy insertion of transgenes in Caenorhabditis elegans. Nat. Genet. *40*, 1375–1383.

Golding, I., Paulsson, J., Zawilski, S.M., and Cox, E.C. (2005). Real-time kinetics of gene activity in individual bacteria. Cell *123*, 1025–1036.

Green, J.L., Inoue, T., and Sternberg, P.W. (2008). Opposing Wnt pathways orient cell polarity during organogenesis. Cell *134*, 646–656.

Harris, J., Honigberg, L., Robinson, N., and Kenyon, C. (1996). Neuronal cell migration in C. elegans: regulation of Hox gene expression and cell position. Development *122*, 3117–3131.

Henrichsen, C.N., Chaignat, E., and Reymond, A. (2009). Copy number variants, diseases and gene expression. Hum. Mol. Genet. *18*(R1), R1–R8.

Hirsch, H.A., Iliopoulos, D., Joshi, A., Zhang, Y., Jaeger, S.A., Bulyk, M., Tsichlis, P.N., Shirley Liu, X., and Struhl, K. (2010). A transcriptional signature and common gene networks link cancer with lipid metabolism and diverse human diseases. Cancer Cell *17*, 348–361.

Hooshangi, S., Thiberge, S., and Weiss, R. (2005). Ultrasensitivity and noise propagation in a synthetic transcriptional cascade. Proc. Natl. Acad. Sci. USA *102*, 3581–3586.

Hornung, G., and Barkai, N. (2008). Noise propagation and signaling sensitivity in biological networks: a role for positive feedback. PLoS Comput. Biol. *4*, e8.

Kalmar, T., Lim, C., Hayward, P., Muñoz-Descalzo, S., Nichols, J., Garcia-Ojalvo, J., and Martinez Arias, A. (2009). Regulated fluctuations in nanog expression mediate cell fate decisions in embryonic stem cells. PLoS Biol. *7*, e1000149.

Kepler, T.B., and Elston, T.C. (2001). Stochasticity in transcriptional regulation: origins, consequences, and mathematical representations. Biophys. J. *81*, 3116–3136.

Kholodenko, B.N., Kiyatkin, A., Bruggeman, F.J., Sontag, E., Westerhoff, H.V., and Hoek, J.B. (2002). Untangling the wires: a strategy to trace functional interactions in signaling and gene networks. Proc. Natl. Acad. Sci. USA *99*, 12841–12846.

Korswagen, H.C. (2002). Canonical and non-canonical Wnt signaling pathways in Caenorhabditis elegans: variations on a common signaling theme. Bioessays *24*, 801–810.

Korswagen, H.C., Herman, M.A., and Clevers, H.C. (2000). Distinct beta-catenins mediate adhesion and signalling functions in C. elegans. Nature *406*, 527–532.

Kussell, E., and Leibler, S. (2005). Phenotypic diversity, population growth, and information in fluctuating environments. Science *309*, 2075–2078.

Lagha, M., Bothma, J.P., and Levine, M. (2012). Mechanisms of transcriptional precision in animal development. Trends Genet. *28*, 409–416.

Levine, M. (2011). Paused RNA polymerase II as a developmental checkpoint. Cell *145*, 502–511.

Li, G.-W., and Xie, X.S. (2011). Central dogma at the single-molecule level in living cells. Nature *475*, 308–315.

Milo, R., Shen-Orr, S., Itzkovitz, S., Kashtan, N., Chklovskii, D., and Alon, U. (2002). Network motifs: simple building blocks of complex networks. Science *298*, 824–827.

Mukhopadhyay, A., Deplancke, B., Walhout, A.J.M., and Tissenbaum, H.A. (2008). Chromatin immunoprecipitation (ChIP) coupled to detection by quantitative real-time PCR to study transcription factor binding to DNA in Caenorhabditis elegans. Nat. Protoc. *3*, 698–709.

Munsky, B., Neuert, G., and van Oudenaarden, A. (2012). Using gene expression noise to understand gene regulation. Science *336*, 183–187.

Nijhout, H.F. (2002). The nature of robustness in development. BioEssays *24*, 553–563.

Niu, W., Lu, Z.J., Zhong, M., Sarov, M., Murray, J.I., Brdlik, C.M., Janette, J., Chen, C., Alves, P., Preston, E., et al. (2011). Diverse transcription factor binding features revealed by genome-wide ChIP-seq in C. elegans. Genome Res. *21*, 245–254.

Ozbudak, E.M., Thattai, M., Lim, H.N., Shraiman, B.I., and Van Oudenaarden, A. (2004). Multistability in the lactose utilization network of Escherichia coli. Nature *427*, 737–740.

Pedraza, J.M., and van Oudenaarden, A. (2005). Noise propagation in gene networks. Science *307*, 1965–1969.

Raj, A., and van Oudenaarden, A. (2008). Nature, nurture, or chance: stochastic gene expression and its consequences. Cell *135*, 216–226.

Raj, A., Peskin, C.S., Tranchina, D., Vargas, D.Y., and Tyagi, S. (2006). Stochastic mRNA synthesis in mammalian cells. PLoS Biol. *4*, e309.

Raj, A., van den Bogaard, P., Rifkin, S.A., van Oudenaarden, A., and Tyagi, S. (2008). Imaging individual mRNA molecules using multiple singly labeled probes. Nat. Methods *5*, 877–879.

Raj, A., Rifkin, S.A., Andersen, E., and van Oudenaarden, A. (2010). Variability in gene expression underlies incomplete penetrance. Nature *463*, 913–918.

Raser, J.M., and O'Shea, E.K. (2004). Control of stochasticity in eukaryotic gene expression. Science *304*, 1811–1814.

Rosenfeld, N., Young, J.W., Alon, U., Swain, P.S., and Elowitz, M.B. (2005). Gene regulation at the single-cell level. Science *307*, 1962–1965.

Salser, S.J., and Kenyon, C. (1992). Activation of a C. elegans Antennapedia homologue in migrating cells controls their direction of migration. Nature *355*, 255–258.

Sato, A., Kojima, T., Ui-Tei, K., Miyata, Y., and Saigo, K. (1999). Dfrizzled-3, a new Drosophila Wnt receptor, acting as an attenuator of Wingless signaling in wingless hypomorphic mutants. Development *126*, 4421–4430.

Shahrezaei, V., and Swain, P.S. (2008). The stochastic nature of biochemical networks. Curr. Opin. Biotechnol. *19*, 369–374.

Sulston, J.E., and Horvitz, H.R. (1977). Post-embryonic cell lineages of the nematode, Caenorhabditis elegans. Dev. Biol. *56*, 110–156.

Taniguchi, Y., Choi, P.J., Li, G.-W., Chen, H., Babu, M., Hearn, J., Emili, A., and Xie, X.S. (2010). Quantifying E. coli proteome and transcriptome with single-molecule sensitivity in single cells. Science *329*, 533–538.

Thattai, M., and van Oudenaarden, A. (2004). Stochastic gene expression in fluctuating environments. Genetics *167*, 523–530.

To, T.-L., and Maheshri, N. (2010). Noise can induce bimodality in positive transcriptional feedback loops without bistability. Science *327*, 1142–1145.

Weinberger, L.S., Burnett, J.C., Toettcher, J.E., Arkin, A.P., and Schaffer, D.V. (2005). Stochastic gene expression in a lentiviral positive-feedback loop: HIV-1 Tat fluctuations drive phenotypic diversity. Cell *122*, 169–182.

Weinberger, L., Voichek, Y., Tirosh, I., Hornung, G., Amit, I., and Barkai, N. (2012). Expression noise and acetylation profiles distinguish HDAC functions. Mol. Cell *47*, 193–202.

Wernet, M.F., Mazzoni, E.O., Celik, A., Duncan, D.M., Duncan, I., and Desplan, C. (2006). Stochastic spineless expression creates the retinal mosaic for colour vision. Nature *440*, 174–180.

Whangbo, J., and Kenyon, C. (1999). A Wnt signaling system that specifies two patterns of cell migration in C. elegans. Mol. Cell *4*, 851–858.

Willert, J., Epping, M., Pollack, J.R., Brown, P.O., and Nusse, R. (2002). A transcriptional response to Wnt protein in human embryonic carcinoma cells. BMC Dev. Biol. *2*, 8.

Wolf, D.M., Vazirani, V.V., and Arkin, A.P. (2005). Diversity in times of adversity: probabilistic strategies in microbial survival games. J. Theor. Biol. *234*, 227–253.

Xiong, W., and Ferrell, J.E., Jr. (2003). A positive-feedback-based bistable 'memory module' that governs a cell fate decision. Nature *426*, 460–465.

Zenklusen, D., Larson, D.R., and Singer, R.H. (2008). Single-RNA counting reveals alternative modes of gene expression in yeast. Nat. Struct. Mol. Biol. *15*, 1263–1271.

Zinovyeva, A.Y., Yamamoto, Y., Sawa, H., and Forrester, W.C. (2008). Complex network of Wnt signaling regulates neuronal migrations during Caenorhabditis elegans development. Genetics *179*, 1357–1371.